Observations and analysis of Alfvén wave phase mixing in the Earth's magnetosphere

T. E. Sarris,[1,2] A. N. Wright,[3] and X. Li[1]

[1]   Signatures of Alfvén wave phase mixing in the Earth's magnetosphere, observed as polarization rotation of a transverse, Pc5 magnetospheric pulsation, are presented and compared to theory. The polarization rotation occurred during a rare event of a dayside narrowband ULF magnetospheric pulsation that lasted for 5 consecutive days, from 24 to 30 November 1997; details of this event were reported by Sarris et al. (2009) through observations at geosynchronous orbit and on the ground. In this paper we investigate the polarization signatures of the pulsation by performing a detailed analysis of its transverse components as observed through hodogram plots. Density measurements from one of the Los Alamos National Laboratory (LANL) spacecraft which had its L shells closest to GOES-8 are used to calculate field line resonance frequencies at geosynchronous orbit; these frequency calculations show good agreement with the observed pulsations but also have a local time offset. For an instance of an observed polarization rotation we estimate the observed poloidal lifetime of the pulsation by the time taken for the poloidal and toroidal amplitudes to become equal, which we compare with the theoretical approximation to the poloidal lifetime, as calculated in a box model magnetosphere by Mann and Wright (1995). Density measurements from different LANL spacecraft at geosynchronous orbit and their varying L shells as derived from their varying local times are used to estimate a local gradient in the local Alfvén speed, which is then used in the calculation of the predicted poloidal lifetime. This is the first time that such polarization rotations are directly observed and compared with theoretical predictions.

1.   Introduction

[2]   Ultralow frequency (ULF) waves in the magnetosphere are considered to be among the candidate sources of electron flux enhancements in the radiation belts. Several theoretical studies have simulated in detail interactions between ULF waves, particularly in the Pc5 range, and radiation belt energetic (MeV) electrons, and have shown that not all classes of ULF waves are equally important for radiation belt electron acceleration: mode structure analysis and simulations by *Hudson et al.* [2000] and *Elkington et al.* [2003] suggest that electrons could be adiabatically accelerated through a drift-resonance interaction with either azimuthal (toroidal) mode or radial (poloidal) mode ULF waves and indicate that, whereas in the nonaxisymmetric outer regions of the magnetosphere both toroidal- and poloidal-mode waves may cause transport in association with the respective radial and azimuthal drift motions of the particle, in the axisymmetric inner regions of the magnetosphere the azimuthal drift is dominant, and low-m-number poloidal modes are more efficient than toroidal modes for bulk acceleration. Thus it is important that the characteristics, interactions and lifetimes of the toroidal and poloidal modes are well understood. To this direction, we report the first observations of poloidal Alfvén waves being converted to toroidal Alfvén waves in the magnetosphere and we discuss through observation and simulation the timing for the observed phase mixing.

[3]   The process of Alfvén wave phase mixing has been discussed in the context of toroidal Alfvén waves in the magnetosphere for several decades [e.g., *Radoski*, 1976]. Phase mixing is a time-dependent process and not readily appreciable in normal mode calculations. Although the existence of normal mode poloidal Alfvén wave solutions have been known for over half a century [*Dungey*, 1954], it was not until relatively recently that the time-dependent behavior of these waves was shown to exhibit phase mixing also [*Mann and Wright*, 1995]. Interestingly, the ideal phase mixing process leads to small scales developing in both toroidal and poloidal Alfvén waves, however, the consequence for the two types of waves is very different: Toroidal waves remain as toroidal waves with increasing fine structure, whereas the fine scales that the poloidal waves develop

[1]Laboratory for Atmospheric and Space Physics, University of Colorado, Boulder, Colorado, USA.
[2]Space Research Laboratory, Democritus University of Thrace, Xanthi, Greece.
[3]School of Mathematics and Statistics, University of St Andrews, Saint Andrews, UK.

across L shells eventually cause them to convert to toroidal waves.

[4] In the theoretical description of ionospheric interaction with magnetospheric pulsations, both the poloidal and toroidal wave components are expected to be heavily damped by driving Pedersen currents in the resistive ionospheric boundaries: a numerical calculation of the ionospheric damping rate of poloidal pulsations by the method of *Newton et al.* [1978] for the first harmonic, on the L shell where the pulsations are observed, gives a damping estimate of $\tau \sim 12$ min for the poloidal lifetime; for the first toroidal harmonic *Allan and Knox* [1979] give an estimate of $\tau \sim 14$ min. Another energy loss mechanism that could lead to the damping of compressional ULF pulsations is the tailward escape of fast-mode energy, following the waveguide geometry [*Wright*, 1994], or the process by which ULF energy is lost into the solar wind [*Fujita and Glassmeier*, 1995; *Lee*, 1996].

[5] Apart from damping, various ways have been described by which an excited pulsation can be altered within the inner magnetosphere. It has been shown by theoretical calculations that low m, externally produced fast poloidal pulsations can resonantly drive a local toroidal field line resonance in the inner magnetosphere, at the point where the frequency of the fast poloidal waves matches the local Alfvén resonance frequency [*Southwood*, 1974; *Chen and Hasegawa*, 1974; *Kivelson and Southwood*, 1985; *Wright and Rickard*, 1995; *Mann and Wright*, 1995]. In the process the energy of the poloidal fluctuation is gradually transferred to toroidal field line resonances. Thus it is expected that poloidal oscillations have a finite lifetime. In a numerical simulation of a box magnetosphere that was performed by *Mann and Wright* [1995] it has been suggested that, not only low-m compressional poloidal waves will gradually decay, being transformed to Alfvén waves, but also large-m MHD poloidal Alfvén waves excited internally in an inhomogeneous plasma will have a finite lifetime, gradually being converted to Alfvén waves of toroidal polarization. Theoretical calculations by *Mann and Wright* [1995] in the box model gave $\tau \sim 13$ min as an estimate of the time before ideal poloidal Alfvén waves become dominantly toroidal for typically observed parameters.

[6] In this paper, observations of phase mixing between toroidal and poloidal Alfvén waves were made during a narrowband Pc5 pulsation event that was observed in the dayside magnetosphere at geosynchronous orbit for five consecutive days over successive passages of GOES-8 and GOES-9 satellites, from 24 to 30 November 1997; the details of this rare event with an unprecedented duration have been reported by *Sarris et al.* [2009]. The event was primarily radially polarized, and the frequency of the pulsation was observed to range from 5 to 9 mHz during the first day, with frequency being higher in the prenoon region; on subsequent days the frequency range of the pulsation narrowed down, until it centered around 5 mHz ± 0.5 mHz one day before diminishing. This event occurred during the recovery phase of a major geomagnetic storm (min Dst = −108nT); the recovery lasted for a few days, during which the solar wind dynamic pressure was rather stable. Geotail measurements in the outer magnetosphere have shown no connection to external pulsations in the solar wind during this event, leading to the speculation that there

is an internal source for these pulsations; it is possible that the poloidal mode is driven by an energetic ion population, in a mechanism similar to the one described by *Chen and Hasegawa* [1991, and references therein]. Ground magnetometers were used to study the radial extent of the pulsations and to calculate the mode number of the pulsations whenever they were observed on the ground; the event was found to be radially confined to within a few R_E around geosynchronous orbit, whereas through measurements of the phase differences between ground stations aligned along similar latitudes the azimuthal mode number was found to range between 20 and 55. The long duration of these pulsations indicated that a driving mechanism must be operating quasi-continuously on the dayside magnetosphere during the entire five day period that the pulsations are observed.

[7] Here we focus on the polarization characteristics of the pulsations and in particular on the evolution of polarization rotation, which we then compare to theoretically predicted times for polarization rotation: through a detailed observation of the poloidal and toroidal components of the ULF wave time series the early phases of mode conversion are observed, with signatures of the rotation from an initially poloidally polarized wave to a circularly polarized (poloidal and toroidal) wave. In the simulations performed by *Mann and Wright* [1995] it is predicted that such polarization rotations will occur in areas of gradients in the local density and a prediction of the time for the polarization rotation is given on the basis of the spatial gradient of the Alfvén frequency. However, such prediction has never been validated by direct observations. At the time that the polarization rotation is observed by GOES, near-simultaneous cold plasma observations from multiple LANL geosynchronous satellites show large variations in density. These satellites are located at different local times and are hence monitoring plasma properties at different L shells, which we use to infer a radial gradient in density and thus a spatial gradient of the Alfvén frequency, as predicted by *Mann and Wright* [1995]. Comparisons between the model prediction and calculations of the polarization rotation time are made on the basis of these observations.

2. Observations

2.1. Geosynchronous Magnetic Field Measurements

[8] Geosynchronous magnetic field measurements from satellites GOES-8 and GOES-9 [*Singer et al.*, 1996] and the corresponding Dynamic Power Spectra (DPS) over the period from 24 to 29 November 1997 were presented by *Sarris et al.* [2009], in which intense transverse pulsations, mostly in the radial but also in the azimuthal direction, were observed to last for 5 days; here in Figure 1a we present in more detail the radial component of the magnetic field data, B_r for the day that the most intense fluctuations were observed, on 25–26 November 2001. In order to separate the ULF field variations perpendicular to as well as along the magnetic field direction, the components of the magnetic field vector are projected in a Mean Field Aligned (MFA) coordinate system. In this system $\widehat{e}_{//}$ points along the average background magnetic field direction and is obtained from a 30-min running average of the instantaneous magnetic field, centered at the data point being processed; $\widehat{e}_{\phi}$ is determined by $\widehat{e}_{//} \times \vec{r}_e$, where $\vec{r}$ is the
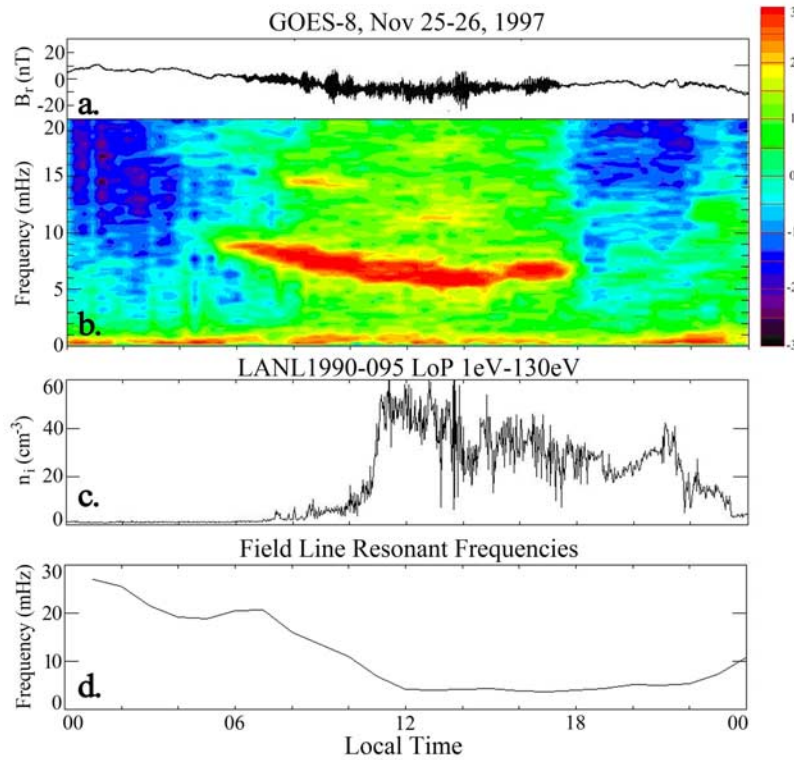
Figure 1. (a) The radial component of the magnetic field, B_r, as measured by GOES-8 from local midnight on 25 November to local midnight on 26 November. (b) The corresponding Dynamic Power Spectra; the color scale corresponds to the logarithm of power in $nT^2\ Hz^{-1}$. (c) Density measurements at geosynchronous orbit on the same day, as observed by LANL 1990-095, which was close to GOES-8 in local time. (d) The field line resonant frequencies, calculated every 1 h in local time by integrating field lines traced in the T96 magnetic field model, assuming a homogeneous density along field lines.

unit vector along the line from the earth to the instantaneous satellite position; and $\widehat{\mathbf{e}}_r$ is obtained by $\widehat{\mathbf{e}}_\phi \times \widehat{\mathbf{e}}_{//}$, completing the orthogonal system. Thus $\widehat{\mathbf{e}}_\phi$ points in the eastward direction and $\widehat{\mathbf{e}}_r$ in the meridional direction, pointing radially outward at the magnetic equator. Waves in the $\widehat{\mathbf{e}}_{//}$, $\widehat{\mathbf{e}}_r$ and $\widehat{\mathbf{e}}_\phi$ directions are referred to as compressional, poloidal and toroidal respectively. In rotating the field components into MFA coordinates, the 30-min average acts as a high pass filter removing frequencies below 0.55 mHz. On this day pulsations were also observed on the ground; from these observations mode number m was calculated to range between 20 and 55, as shown by *Sarris et al.* [2009]. In Figure 1b the Dynamic Power Spectra (DPS) of B_r, the radial component of the magnetic field data are plotted. The DPS calculations were performed by sliding a Hanning window through the data and performing a Fast Fourier Transform (FFT) on the subset of the signal within the window. For a 0.512-s sampling frequency, the Nyquist frequency (and hence the maximum frequency we can monitor in this data set) is 976 mHz; in order, however, to better show the fluctuations in the Pc5 range, only frequencies up to 20 mHz are shown in Figure 1b.

2.2. Geosynchronous Ion Density Measurements

[9] Plasma density affects significantly the occurrence and frequency characteristics of magnetospheric pulsations.

Shear Alfvén waves in the magnetosphere, whether generated externally or internally, will have predictable frequencies that depend on plasma density, the magnetic field strength and the length of field lines in the vicinity of the fluctuations. Plasma density measurements for this event were acquired by the Magnetospheric Plasma Analyzer (MPA) instruments built by the Los Alamos National Laboratory (LANL) and flown on geosynchronous satellites 1994-084, LANL-97A and 1990-095; the locations of these satellites together with the locations of GOES-8 and GOES-9 at 1200 UT every day are marked in Figure 2 (left), in GSE coordinates. The different longitudes of the three spacecraft, as shown in Figure 2 (left), cause them to have different angles with respect to the direction of the Earth's dipole moment, and thus to monitor different L shells when they cross the same local time. The field lines through the LANL and GOES satellites when the satellites cross local noon are plotted in Figure 2 (right), on the X-Z plane, also in GSE coordinates. The position of minimum B along the traced field lines is marked with a square; geosynchronous orbit is also plotted. Field lines in Figure 2 (right) were traced using the T96 magnetic field model [*Tsyganenko*, 1995], using as input parameters the magnetospheric and solar wind conditions on this day. These conditions were a *Dst* index of -25 nT, solar wind ram pressure of 1.3 nP, IMF $B_y = -5$ and $B_z = 3.0$. Calculations of the L shell of
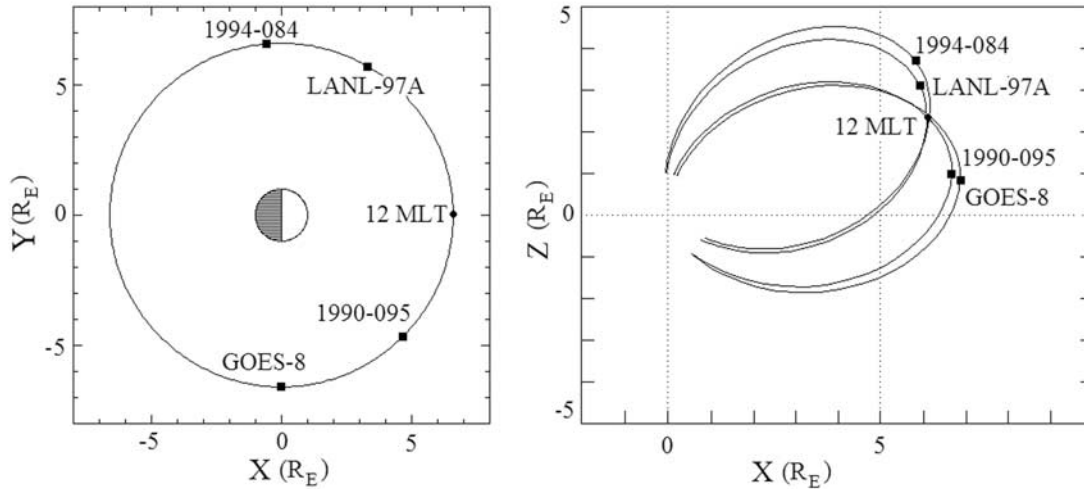
Figure 2. (left) The local time separation of the LANL and GOES-8 geosynchronous satellites, 1200 UT, results in variable angles with respect to the direction of the Earth's dipole moment and the monitoring of variable L shells. (right) The field lines through the satellites when they cross local noon (marked 12 MLT), calculated using the T96 magnetic field model. The location of minimum B for each field line is marked with a black square. Minimum B values along the field lines indicate that 1990-095 is located inward, followed by GOES-8, LANL-97A, and 1994-084, which is located farther out in the L shell.

GOES and the three LANL geosynchronous satellites were also performed using the T96 magnetic field model [*Tsyganenko*, 1995], through the SPENVIS interface provided by ONERA [*Heynderickx et al.*, 2000] (see http://www.spenvis.oma.be/spenvis/). The input parameters used were the solar wind conditions on 25–26 November 1997, as listed above. The L shells of the LANL satellites at the local time where the polarization rotations were observed are: 1990-095: $L = 7.0$; LANL-97A: $L = 7.1$; and 1994-084: $L = 7.4$. The variation in L between satellites on the same orbit arising because of the longitudinal separation of the spacecraft and the resulting variable angles with respect to the magnetic axis of the Earth has been described in detail by *Onsager et al.* [2004], who estimated ΔL between GOES-8 and GOES-9 to vary between 0.5 and 1 during quiet magnetospheric conditions.

[10] Low-energy plasma number density measurements from the LoP energy channel ($\sim$1eV to 130eV) of the MPA instrument on the three Los Alamos satellites 1990-095, 1994-084 and LANL-97A are plotted as a function of local time in Figure 3. In Figure 3 the vertical lines indicate local midnight crossings of the satellites. The dates marked correspond to the dates the satellites cross local noon. A significant variation in density can be observed between the three LANL spacecraft that provided low-energy plasma measurements at that time, with satellite LANL 1990-095, located inward of the other LANL satellites, generally measuring larger densities in the noon and postnoon region. Taking into account the L shell calculations described above, these plasma measurements indicate a sharp inward gradient in density around the noon and postnoon regions. We note here that cold plasma dominates total number density measurements, and that the measurements presented in Figure 3 are a first-order approximation of total density,

which is nevertheless sufficient for the purposes of this study.

[11] In order to compare the local magnetic field conditions at each satellite's location, the following parameters are listed in Table 1: in the first five columns the satellite names, longitude (GLon), magnetic latitude (MLat), universal time (UT) and L shell are listed for local time 1400, which is the local time that the polarization rotation discussed in section 3.2 is observed. On the sixth column, density measurements for the three LANL satellites on 25 November 1997 are shown, averaged over a 1-h interval around the local time of interest. On the last three columns the local Alfvén speed υ_A, field line resonance (FLR) cyclic frequency f_A, and angular frequency ω_A are listed, calculated from the local measured density and the modeled B_{min} strength; these calculations are discussed in the next section.

[12] From the measurements and L shell calculations that are presented in Table 1, a clear inward gradient in density can be observed, consistently for all three LANL spacecraft that are providing density measurements, with the most inward of the three satellites, 1990-095 ($L = 7.0$) measuring higher density, followed by LANL-97A ($L = 7.1$) and by 1994-084, which is located further out in L ($L = 7.4$) and measures the lowest density. In section 3.1 we use the density as measured by satellite 1990-095, which was located the closest to GOES-8 together with model magnetic field strength along the field line through the location of satellite GOES-8 to calculate the FLR frequency on 25 November, the day of strongest fluctuations; we show that the calculated FLR frequency in the dayside is close to the frequency of the pulsations measured by GOES-8. In section 3.2 we plot hodograms of the observed magnetic field components and show an interval of polarization rotation, from which the characteristic time for polarization rotation is estimated. These hodograms are compared with the theoret-
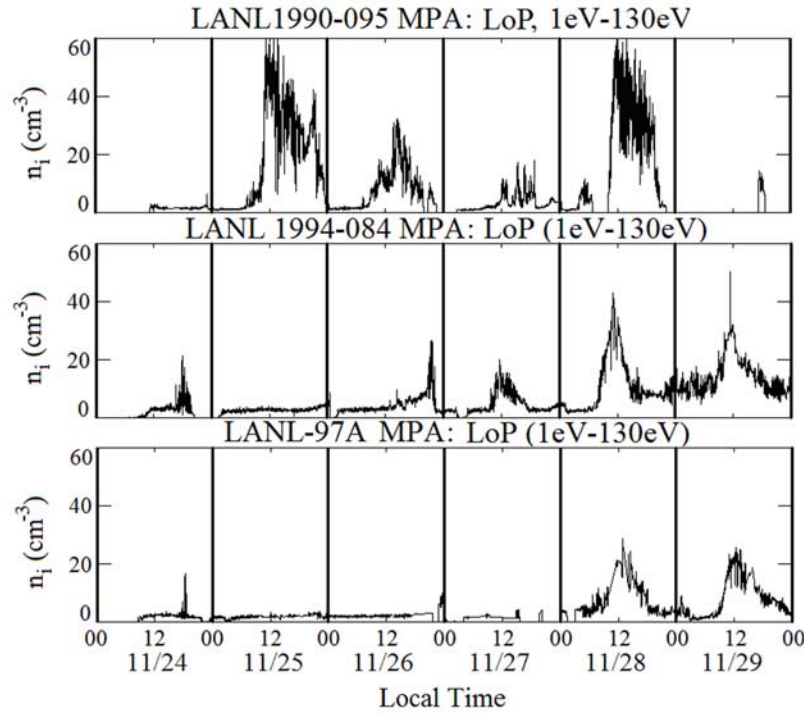
Figure 3. Plasma density (protons) from the LoP energy channel (1–130 eV) of the MPA instrument on three LANL geosynchronous satellites from 24 to 30 November 1997. Combined with L shell estimates, these measurements indicate a radially inward density gradient. Satellite 1990-095 is located on inner L shells and is the closest to the L shells through the GOES-8 location.

ical predictions of polarization rotation by *Mann and Wright* [1995]. In section 3.3 we further discuss the implications of density and local FLR frequency variations, and compare the observed time for polarization rotation to theoretical estimates based on an idealized model magnetosphere.

3. Discussion

3.1. Local Density, Alfvén Speed, and Field Line Resonances

[13] Plasma density can be used to calculate the local Alfvén velocity, $v_A = B (\mu_0 \rho)^{-1/2}$, where B is the magnitude of the magnetic field, $\rho = n_i m_i$ is the plasma mass density, n_i is the ion number density, m_i is the mass of H^+ ions (all ions are assumed to be H^+ here), and μ_0 is the magnetic permeability of space. The Alfvén velocity can in turn be used to calculate the local FLR frequency and period of the fluctuations by integration along a field line, using $T = 1/f = 2\int 1/v_A \, ds$ as an estimate for the FLR period [*Obayashi and*

Jacobs, 1958]. In order to calculate the local FLR frequency at GOES-8 locations we integrated field lines passing through GOES-8 orbit from the T96 magnetic field model [*Tsyganenko*, 1995] and used plasma number density measurements from the LoP energy channel (energies ~1eV to 130eV) of MPA instrument on satellite LANL 1990-095, which traverses L shells closest to GOES-8. Field lines were traced every 1 h in local time from locations along GOES-8 orbit, and density measurements from satellite LANL 1990-095 were averaged every 1 h in local time.

[14] In Figure 1d we plot the calculated FLR frequencies for the same local times as the magnetic field data shown in Figure 1a. From Figure 1d it can be seen that, at the time of increased density at LANL 1990-095, the calculated FLR frequency is within the frequency range of the GOES-8 narrowband pulsation, reinforcing the understanding that the narrowband pulsations are FLRs. An offset of about 5 h in local time is observed between magnetic field and density measurements, with LANL 1990-095 observing high densities shifted toward the afternoon regions com-

Table 1. Local Properties of Magnetic Field Lines at Geosynchronous Orbit at 1400 LT[a]

Satellite	GLon	MLat	Universal Time	L Shell	n_i (cm^{-3})	v_A (km s^{-1})	f_A (mHz)	ω_A (rad s^{-1})
GOES-8	285°	10.5°	1900	7.1	—	—	—	—
1990-095	323°	8.7°	1628	7.0	46	320	3.7	0.024
LANL-97A	70°	−8.4°	0708	7.1	3.8	920	10	0.065
1994-084	103°	−10.6°	0918	7.4	2.5	1000	11	0.068

[a]The geographic longitude (GLon), magnetic latitude (MLat), universal time, and L shell of satellites GOES-8, 1990-095, LANL-97A, and 1994-084 when they cross local time 1400, are listed in the second through fifth columns, respectively. The sixth column lists density measurements for the three LANL satellites on 25 November 1997, averaged over a 1-h interval around local noon. The seventh column lists the calculated local Alfvén velocity, v_A (in km s^{-1}), based on local LANL density measurements and on model estimates of B_{min}. The eighth and ninth columns give the field line resonance cyclic frequency, f_A (in mHz), and angular frequency, ω_A (in rad s^{-1}).
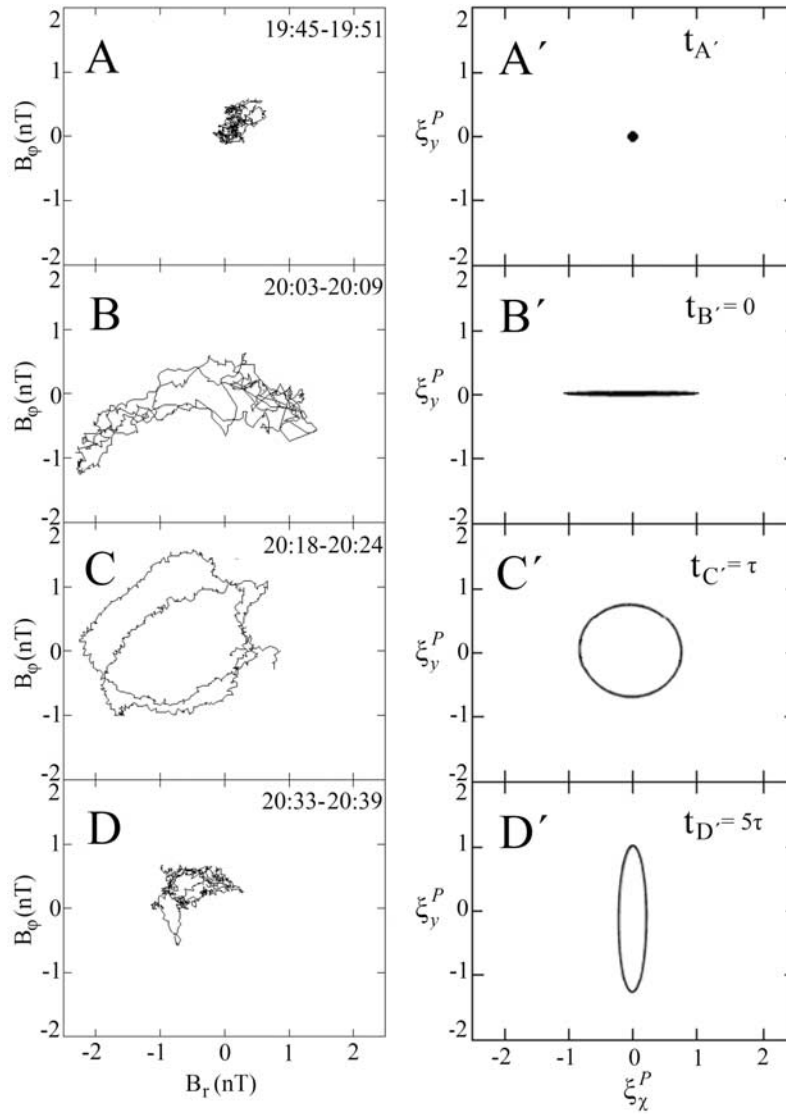
Figure 4. (left) The toroidal component of the magnetic field, B_φ, is plotted versus the poloidal component, B_r, for four 6-min intervals of day 330 (26 November) 1997, marked A through D, corresponding to intervals A through D in Figure 5. Following a period of no pulsations (interval A), a purely poloidal pulsation is initiated (interval B), followed by a circular hodogram (interval C) which eventually diminishes (interval D). (right) The theoretical evolution of the polarization of a pulsation is plotted, adapted from *Mann and Wright* [1995, Figure 5]. Here τ is the poloidal lifetime and ξ_x^P and ξ_y^P are the physical plasma displacements in the simulation of *Mann and Wright* [1995]. A purely toroidal pulsation, such as that shown in interval D′ is not observed in interval D.

pared to the fluctuations at GOES-8. This could be due to the separation in L shell between the two spacecraft: It is possible that the high-density region, with which we associate the narrowband fluctuations, has an asymmetry toward evening local times.

[15] In calculations of the local FLR frequencies we assumed that ion number density remains constant along a field line, even though an increase is expected as one encounters the F region. However, we note that the increase in magnetic field strength will cause the integrand to diminish close to the field line foot points, where density increases significantly. Physically, the time period is determined by the time the Alfvén waves take to traverse the low

Alfvén speed (equatorial) section of the tube, not the high Alfvén speed region near the Earth. Another simplifying assumption in this calculation is that all ions are assumed to be protons, as the LANL-MPA instrument does not have the capability of distinguishing among ion species: even though heavy ions are present in the inner magnetosphere, we assume here that composition is dominated by protons. We also note here that the WKB approximation used in calculating the resonant frequency is not the most accurate: *Taylor and Walker* [1984] and *Wright et al.* [2002] compared the WKB approximation to other approximations, such as the one used by *Taylor and Walker* [1984], and estimated that the error when using the WKB approximation
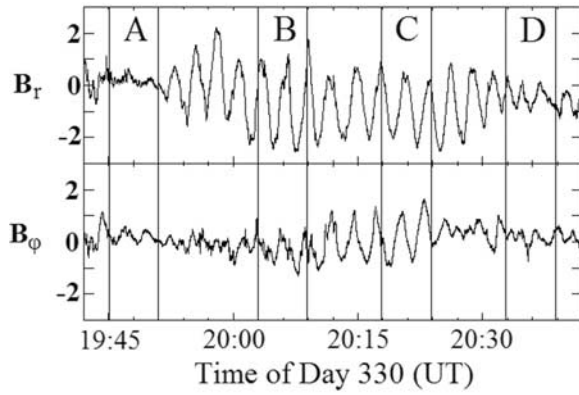
Figure 5. The poloidal and toroidal components of GOES-8 magnetic field, B_r and B_φ, are plotted in time for 1 h of day 330 (26 November) 1997. The polarization rotation occurs through intervals B, C, and D.

for the fundamental frequency is about 10 percent, whereas for the second harmonic the error is expected to be a few percent. However, these errors are acceptable for the purposes of the calculations made in this paper.

3.2. Hodograms

[16] As discussed in section 1, large-m MHD poloidal Alfvén waves excited internally in inhomogeneous plasma are expected to have a finite lifetime. This has been demonstrated in an MHD simulation of an idealized box model magnetosphere by *Mann and Wright* [1995]. In this simulation it has been shown that an initially (large m) Alfvén wave with predominantly poloidal polarization, when oscillating in an inhomogeneous plasma, asymptotically approaches a purely toroidal polarization state over a predictable timescale. The conversion of poloidal to toroidal fields was demonstrated in the simulation through a hodogram plot of the transverse components of the fluctuating magnetic field. This is shown schematically in Figure 4 (right), in which an initially linear fluctuation in the purely poloidal direction (interval B′) gradually mixes with the toroidal component, shown as a circle in the hodogram (interval C′), and finally is converted to a purely toroidal fluctuation (interval D′). As noted by Mann and Wright, this signature requires that the poloidal waves stop being driven by the internal generation mechanism after the initial excitation. If the excitation mechanism remains active it is expected that an initial linearly polarized pulsation will be succeeded by a mixed pulsation, and that the purely toroidal mode will not be observed. In the event reported herein the pulsations last for days, much longer than the theoretically calculated damping times; thus we find it most reasonable to assume that the pulsations are continuously driven for the duration of the event. It is possible that the slow decay of the ring current ions during the recovery phase after the storm as described above and also by *Sarris et al.* [2009] provided the energy for the sustained ULF waves, via drift-bounce resonance.

[17] By plotting the poloidal versus the toroidal components of the magnetic field data and monitoring them for the entire 5-day duration of the event, several instances of the early stages of polarization conversion were observed, where an initially purely poloidal pulsation eventually

becomes circularly polarized, without being converted to a purely toroidal polarization. This feature is an indication of an excitation mechanism that remains active. A plot of such an instance is given in Figure 5: the poloidal and toroidal magnetic field components, $\mathbf{B_r}$ and $\mathbf{B_\varphi}$ respectively are plotted in time for 1 h of day 330 (26 November), when GOES-8 was located in the early afternoon region ($\sim$1400 local time). In the left four plots of Figure 4, marked A through D, the toroidal component is plotted versus the poloidal for four 6-min intervals, marked accordingly in the two upper plots. It can be seen that, following a period of small-amplitude pulsations (interval A), a $\sim$4 nT peak-to-peak, mostly poloidal pulsation is initiated (interval B). About 10 to 15 min later the pulsation is of equal magnitude in the poloidal and the toroidal directions, as shown in the circular hodogram in the next plot (interval C). However, a purely toroidal pulsation is not observed for this time interval. In the survey performed in the whole 5-day period, most of the time the hodograms were random, showing no particular polarization pattern; however linearly polarized fluctuations were often observed, and in few instances they were followed by a clear circular hodogram, similar to interval C of Figure 4. In the whole 5-day period a complete polarization rotation was not positively identified.

3.3. Calculation of Model Polarization Rotation Time

[18] The process that appears to operate in Figures 4 and 5 may be viewed as a poloidal Alfvén wave being driven in a quasi-steady fashion. These waves phase mix and achieve a similar toroidal amplitude after a time given by

$$\tau_p = \lambda/(d\omega_A/dx) \tag{1}$$

Here $\omega_A(x)$ is the local Alfvén frequency, x is the radial coordinate and λ the azimuthal wave number. At later times the ideal calculations of *Mann and Wright* [1995] and *Mann et al.* [1997] show the fields are dominated by the toroidal components. The latter is not observed in our data, and may be understood by including ionospheric dissipation.

[19] Suppose the Alfvén waves drive Joule dissipation in the ionosphere and as a result decay on a timescale of τ_I. We can now identify three classes of solution.

[20] 1. In the case $\tau_I \ll \tau_p$, the poloidal Alfvén waves decay relatively quickly, and do not survive long enough to phase mix. The wave polarization remains poloidal.

[21] 2. In the case $\tau_I \sim \tau_p$, the poloidal fields survive long enough to phase mix and produce toroidal Alfvén waves of a similar amplitude before decaying. The waves have circular polarization.

[22] 3. In the limit $\tau_I \gg \tau_p$, the waves survive for such a long time that phase mixing is sufficient to give a phase mixing length much less than the azimuthal wavelength. Energy that is supplied initially to poloidal fields accumulates as toroidal fields and remains there until dissipated in the ionosphere. These waves have a toroidal polarization.

[23] It is interesting to note that we do not observe high-m toroidal Alfvén waves, suggesting that τ_I is never greater than τ_p. However, we do observe poloidal Alfvén waves and also circularly polarized waves. In the latter case (e.g., interval C in Figure 4) the poloidal wave grew and became established by 1957 UT, and then appears to be driven quasi-steadily until around 2027 UT. During this period the

toroidal fields grew, and a circular polarization was achieved by 2018 UT, suggesting τ_p = 21 min (1957–2018 UT).

[24] Given that the waves in interval C of Figures 4 (left) and 5 are circularly polarized, we expect that $\tau_I \sim \tau_p$. The value of τ_I can be estimated from the analysis by *Allan and Knox* [1979] using their equation (A2) which may be rewritten as

$$\frac{1}{\tau_I} = \frac{A_0}{2LR_EZ_0} \ln\left|\frac{\Sigma_p - a_p^{cr}}{\Sigma_p + a_p^{cr}}\right| \qquad (2)$$

where A_0 is the equatorial Alfvén speed (585 km s^{-1}), Z_0 = cos (θ_0), with θ_0 being the invariant colatitude (23.1° for L = 6.5), Σ_p is the height-integrated ionospheric Pedersen conductivity (10 mho) [see *Wallis and Budzinski*, 1981], and a_p^{cr} = 1/(2 μ_0 A_0 Z_0). These values suggest τ_I = 14 min. An alternative estimate may be found using the results reported by *Newton et al.* [1978, Figure 13]. For L = 6 and Σ_p = 1013 e.s.u., they find τ_I = 14 min, which is consistent with the Allan and Knox estimate allowing for the two models having different density distributions and slightly different L shell values. Given that these models indicate τ_I is about 14 min, and the data in Figures 4 and 5 shows τ_p = 21 min, it does indeed appear that we have a situation in which $\tau_p \sim \tau_I$, which is also in accord with the presence of a circular polarization.

[25] The above analysis gives confidence that $\tau_p \sim$ 20 min, and can be used to infer an Alfvén frequency gradient using equation (1) which may then be compared with observations. Noting that, in the equatorial plane, the azimuthal wavelength is $\lambda = m/L \cdot R_E$ and $dx = R_E \cdot dL$, equation (1) may be rewritten as

$$\frac{d\omega_A}{dL} = \frac{m}{L\tau_p} \qquad (3)$$

[26] Taking L = 7.0, τ_p = 20 min and m = 55 [see *Sarris et al.*, 2009], equation (3) gives $d\omega_A/dL$ = 0.007 s^{-1}L^{-1}. Note that the ground-based measurement of m they reported was actually measured in the prenoon region on the previous day to the GOES-8 data. We assume that this value of m is indicative of the m values of the waves that GOES-8 encountered.

[27] In a fashion similar to the calculations described in section 3.1, we calculated the local FLR frequency at the three LANL satellites when they crossed the local time that the polarization rotation of section 3.2 was observed, using density measurements from the identical MPA instruments on the three satellites and tracing field lines from the location of each LANL satellite. The calculated cyclic and angular frequencies are listed above in the eighth and ninth columns of Table 1. In these calculations a sharp gradient in the Alfvén velocity can be seen, because of the sharp gradient observed in density measurements from the three LANL satellites: As seen in Figure 2, although the three LANL satellites are located in the geographic equatorial plane, their separation in local time results in a geomagnetic latitude difference because of the tilt of the magnetic dipole of the Earth toward Greenland. This will cause the three satellites to monitor different L shells, and thus different

plasma populations. Thus from the cyclic frequency and L shell estimate as given in Table 1 we can calculate the value for $d\omega_A/dL$ as being derived on the basis of density measurements and model calculations of the magnetic field and L shell at the spacecraft location; these calculations yield a value of ~0.010 s^{-1}L^{-1} between satellites LANL-97A and 1994-084 and a value of ~0.087 s^{-1}L^{-1} between satellites 1994-084 and 1990-095. This suggests that there can be considerable variation in the local Alfvén frequency gradient, with values from 0.010 to 0.087 s^{-1}L^{-1} being typical. The value we inferred ($d\omega_A/dL$ = 0.007 s^{-1}L^{-1}) indicates that the gradient at GOES-8 was at the lower end of this range.

4. Summary and Conclusions

[28] By plotting snapshots of the pulsation's hodogram throughout the whole event several instances of polarization mixing were observed, with features similar to the initial phases of polarization rotation; that is, an initially radially polarized pulsation was gradually mixed with the azimuthal component, becoming circularly polarized. A full polarization rotation from a purely poloidal to a purely toroidal pulsation was demonstrated through MHD simulations by *Mann and Wright* [1995]; in the example of polarization mixing that was presented, as well as in all instances of polarization mixing observed in the 5-day period, a full rotation of the pulsations could not be distinguished. This reinforces the speculation that the poloidal pulsations are continuously generated in this event. Ionospheric damping prevents the waves from realizing the asymptotic state of purely toroidal polarization predicted by Mann and Wright.

[29] Plasma measurements at the region where the pulsations were observed were acquired from three LANL geosynchronous satellites; these measurements varied significantly between the three satellites, indicating a sharp inward radial gradient in plasma density. This was explained in terms of the variable L shell that is traversed by the three satellites, because of their separation in longitude. Density measurements from the LANL satellite closest to GOES-8 together with the T96 magnetic field model were used to estimate the local field-line resonant frequency. Good agreement was found between the calculated resonant frequency and the observed narrowband pulsation, even though a local time offset was also observed.

[30] The calculated spatial gradients of acquired plasma densities were used to estimate the theoretically predicted time constant for the rotation from purely poloidally polarized waves to toroidal waves. Observations were then compared to the theoretical estimated time for polarization rotation. Comparison between theoretical and measured polarization rotation times is consistent with a large-m poloidal Alfven wave where the phase mixing time for the polarization rotation to toroidal is similar to the decay time of the wave, resulting in a circular polarization. To our knowledge this is the first time that such a polarization rotation is directly observed and compared to theory, and that the results of the simulations by *Mann and Wright* [1995] are validated by actual observations.

References

Allan, W., and F. B. Knox (1979), The effect of finite ionosphere conductivities on axisymmetric toroidal Alfvén wave resonances, *Planet. Space Sci.*, *27*, 939, doi:10.1016/0032-0633(79)90024-2.

Chen, L., and A. Hasegawa (1974), A theory of long-period magnetic pulsations: 1. Steady state excitation of field line resonance, *J. Geophys. Res.*, *79*, 1024, doi:10.1029/JA079i007p01024.

Chen, L., and A. Hasegawa (1991), Kinetic theory of geomagnetic pulsations: 1. Internal excitations by energetic particles, *J. Geophys. Res.*, *96*, 1503, doi:10.1029/90JA02346.

Dungey, J. W. (1954), Electrodynamics of the outer atmosphere, *Sci. Rep. 69*, Ionos. Res. Lab., Pa. State Univ., University Park.

Elkington, S. R., M. K. Hudson, and A. A. Chan (2003), Resonant acceleration and diffusion of outer zone electrons in an asymmetric geomagnetic field, *J. Geophys. Res.*, *108*(A3), 1116, doi:10.1029/2001JA009202.

Fujita, S., and K.-H. Glassmeier (1995), Magnetospheric cavity resonance oscillations with energy flow across the magnetopause, *J. Geomagn. Geoelectr.*, *47*, 1277.

Heynderickx, D., B. Quaghebeur, E. Speelman, and E. Daly (2000), ESA's space environment information system (SPENVIS): A WWW interface to models of the space environment and its effects, paper presented at 38th Aerospace Sciences Meeting and Exhibit, Am. Inst. of Aeronaut. and Astronaut., Reno, Nev., 10–13 Jan.

Hudson, M. K., S. R. Elkington, J. G. Lyon, and C. C. Goodrich (2000), Increase in relativistic electron flux in the inner magnetosphere: ULF wave mode structure, *Adv. Space Res.*, *25*, 2327, doi:10.1016/S0273-1177(99)00518-9.

Kivelson, M. G., and D. J. Southwood (1985), Resonant ULF waves: A new interpretation, *Geophys. Res. Lett.*, *12*, 49, doi:10.1029/GL012i001p00049.

Lee, D.-H. (1996), Dynamics of MHD wave propagation in the low-latitude magnetosphere, *J. Geophys. Res.*, *101*, 15,371, doi:10.1029/96JA00608.

Mann, I. R., and A. N. Wright (1995), Finite lifetimes of ideal poloidal Alfvén waves, *J. Geophys. Res.*, *100*, 23,677, doi:10.1029/95JA02689.

Mann, I. R., A. N. Wright, and A. W. Hood (1997), Multiple-timescales analysis of ideal poloidal Alfvén waves, *J. Geophys. Res.*, *102*, 2381, doi:10.1029/96JA03034.

Newton, R. S., D. J. Southwood, and W. Hughes (1978), Damping of geomagnetic pulsations by the ionosphere, *Planet. Space Sci.*, *26*, 201, doi:10.1016/0032-0633(78)90085-5.

Obayashi, T., and J. A. Jacobs (1958), Geomagnetic pulsations and the Earth's outer atmosphere, *Geophys. J. R. Astron. Soc.*, *1*, 53.

Onsager, T. G., A. A. Chan, Y. Fei, S. R. Elkington, J. C. Green, and H. J. Singer (2004), The radial gradient of relativistic electrons at geosynchronous orbit, *J. Geophys. Res.*, *109*, A05221, doi:10.1029/2003JA010368.

Radoski, H. R. (1976), Hydromagnetic waves: Temporal development of coupled modes, *Environ. Res. Pap. 559*, Air Force Geophys. Lab., Hanscom Air Force Base, Mass.

Sarris, T., X. Li, and H. J. Singer (2009), A long-duration narrowband Pc5 pulsation, *J. Geophys. Res.*, *114*, A01213, doi:10.1029/2007JA012660.

Singer, H. J., L. Matheson, R. Grubb, A. Newman, and S. D. Bouwer (1996), Monitoring space weather with GOES magnetometers, in *GOES-8 and Beyond*, edited by E. R. Washwell, *Proc. SPIE Int. Soc. Opt. Eng.*, *2812*, 299–308.

Southwood, D. J. (1974), Some features of field line resonances in the magnetosphere, *Planet. Space Sci.*, *22*, 483, doi:10.1016/0032-0633(74)90078-6.

Taylor, J. P. H., and A. D. M. Walker (1984), Accurate approximate formulae for toroidal standing hydromagnetic oscillations in a dipolar geomagnetic field, *Planet. Space Sci.*, *32*, 1119, doi:10.1016/0032-0633(84)90138-7.

Tsyganenko, N. A. (1995), Modeling the Earth's magnetospheric magnetic field confined within a realistic magnetopause, *J. Geophys. Res.*, *100*, 5599, doi:10.1029/94JA03193.

Wallis, D. D., and E. E. Budzinski (1981), Empirical models of height integrated conductivities, *J. Geophys. Res.*, *86*, 125, doi:10.1029/JA086iA01p00125.

Wright, A. N. (1994), Dispersion and wave coupling in inhomogeneous MHD waveguides, *J. Geophys. Res.*, *99*, 159, doi:10.1029/93JA02206.

Wright, A. N., and G. J. Rickard (1995), A numerical study of resonant absorption in a magnetohydrodynamic cavity driven by a broad-band spectrum, *Astrophys. J.*, *444*, 458, doi:10.1086/175620.

Wright, A. N., W. Allan, M. S. Ruderman, and R. C. Elphic (2002), The dynamics of current carriers in standing Alfvén waves: Parallel electric fields in the auroral acceleration region, *J. Geophys. Res.*, *107*(A7), 1120, doi:10.1029/2001JA900168.

————————————

X. Li, Laboratory for Atmospheric and Space Physics, University of Colorado, Boulder, CO 80302, USA.

T. E. Sarris, Space Research Laboratory, Democritus University of Thrace, GR-67100 Xanthi, Greece. (tsarris@ee.duth.gr)

A. N. Wright, School of Mathematics and Statistics University of St Andrews, North Haugh, Saint Andrews KY16 9SS, UK.